A Dynamical Scalar Field Model for Dark Energy: Addressing the Hubble Tension and Cosmic Evolution

Arpit Kottur^{a,1} Jui Mahajan^a and Raka Dabhade^a

 $^a\mathrm{Department}$ of Physics, Fergusson College (Autonomous), Pune, India

Abstract. We propose a dynamical dark energy model based on a canonical scalar field with a hybrid potential of the form $V(\phi) = V_0 e^{-\lambda \phi} + V_1 \phi^n$. We constrain the model's 11-dimensional parameter space using a comprehensive combination of cosmological data, including the Planck 2018 Cosmic Microwave Background (CMB) power spectra, Baryon Acoustic Oscillations (BAO), the Pantheon+ supernova sample, and the matter power spectrum from SDSS. The model provides an excellent fit to the data, with a reduced chi-squared of $\chi^2_{\rm red} = 0.987$, while successfully alleviating the Hubble constant tension. Our analysis yields a Hubble constant of $H_0 = 70.0 \ {\rm km/s/Mpc}$, reducing the discrepancy between early and late-universe measurements. The data favor a negative power-law index of $n \approx -0.92$. A model comparison using the Bayesian Information Criterion finds that the standard Λ CDM model is still slightly preferred (Δ BIC = 2.178) due to its fewer parameters. Nevertheless, our results demonstrate that this hybrid potential model is a compelling, physically motivated alternative to a cosmological constant.

¹Corresponding author.

\mathbf{C}_{0}	ontents	
1	Introduction	1
2	The Scalar Field Model	2
3	Data and Methodology	3
	3.1 Computational Framework	3
	3.2 Observational Data	4
	3.3 Parameter Estimation and Model Comparison	4
4	Results	5
	4.1 Parameter Constraints	5
	4.2 Model Comparison	7
	4.3 Concordance with Cosmological Probes	8
5	Discussion	10
6	Conclusion and Future Work	10
\mathbf{A}	Full Parameter Constraints	11
В	MCMC Convergence Diagnostics	12

1 Introduction

The standard model of cosmology, the Lambda-Cold Dark Matter (Λ CDM) model, has achieved remarkable success in describing a wide range of cosmological observations. It posits a universe dominated by a cosmological constant, Λ , which drives the current phase of accelerated expansion [1, 2], and a non-baryonic, non-relativistic component known as cold dark matter. This framework provides an excellent fit to the temperature and polarization anisotropies of the Cosmic Microwave Background (CMB) as measured by the Planck satellite [3], the distribution of large-scale structure (LSS) [4], and the luminosity distances of Type Ia supernovae.

Despite its successes, the Λ CDM model is beset by persistent challenges, both observational and theoretical. On the theoretical side, the observed value of the cosmological constant is famously fine-tuned, being about 120 orders of magnitude smaller than predictions from quantum field theory [5, 6]. This discrepancy, coupled with the "cosmic coincidence" problem—why the energy densities of matter and dark energy are comparable today—motivates the exploration of alternative theories.

Observationally, the most significant challenge has emerged as a statistically significant tension in the measured value of the Hubble constant, H_0 . Measurements from the local universe, primarily from the SH0ES team using Cepheid-calibrated supernovae, yield a value of $H_0 = 73.04 \pm 1.04 \,\mathrm{km \ s^{-1} Mpc^{-1}}$ [7]. In contrast, the value inferred from early-universe physics, specifically the CMB data from Planck within the Λ CDM framework, is $H_0 = 67.4 \pm 0.5 \,\mathrm{km \ s^{-1} Mpc^{-1}}$ [3]. This discrepancy now stands at the $\sim 5\sigma$ level and suggests

either new physics beyond the standard model or unaccounted-for systematic errors in one or both measurements [8].

One of the most compelling theoretical alternatives to a rigid cosmological constant is the concept of a dynamical dark energy, often modeled as a slowly rolling scalar field, or "quintessence" [9–11]. In such models, the potential energy of the scalar field drives the cosmic acceleration, allowing for an equation of state, w(z), that evolves with time. This dynamical nature offers a potential pathway to resolving the H_0 tension by altering the expansion history of the universe.

A variety of scalar field potentials have been studied in the literature. Exponential potentials, of the form $V(\phi) \propto e^{-\lambda \phi}$, arise naturally in the context of string theory and can produce "tracker" solutions where the scalar field energy density scales with the background radiation or matter density for a period [12]. Power-law potentials, $V(\phi) \propto \phi^n$, have also been extensively explored as a simple and effective parameterization [13].

In this work, we propose and constrain a novel dark energy model driven by a scalar field with a hybrid potential that combines these two well-motivated forms: $V(\phi) = V_0 e^{-\lambda \phi} + V_1 \phi^n$. This framework provides a richer phenomenology, allowing for distinct evolutionary behavior at different cosmic epochs. We implement this model in the Boltzmann solver hi_CLASS and constrain its parameters using a combination of recent cosmological data sets, including Planck 2018 CMB data, Hubble parameter measurements from cosmic chronometers, and the matter power spectrum from the Sloan Digital Sky Survey (SDSS). We show that this model provides an excellent fit to the data and, crucially, offers a promising avenue for alleviating the Hubble tension.

This paper is organized as follows. In Sec. 2, we describe the theoretical framework of our scalar field model. In Sec. 3, we detail the data and statistical methodology used for our analysis. We present our main findings, including parameter constraints and model comparisons, in Sec. 4. We discuss the implications of our results in Sec. 5 and conclude with a summary and directions for future work in Sec. 6.

2 The Scalar Field Model

We model dark energy as a canonical scalar field, ϕ , minimally coupled to gravity. The action for this system in the presence of standard matter components (\mathcal{L}_m) is given by

$$S = \int d^4x \sqrt{-g} \left[\frac{M_{\rm pl}^2}{2} R - \frac{1}{2} g^{\mu\nu} \partial_{\mu} \phi \partial_{\nu} \phi - V(\phi) + \mathcal{L}_m \right], \tag{2.1}$$

where g is the determinant of the metric tensor $g_{\mu\nu}$, R is the Ricci scalar, and $M_{\rm pl} = (8\pi G)^{-1/2}$ is the reduced Planck mass. The dynamics of the field are determined by its potential, $V(\phi)$. We propose a hybrid potential that combines a quintessential exponential term with a power-law term:

$$V(\phi) = V_0 e^{-\lambda \phi} + V_1 \phi^n, \tag{2.2}$$

where V_0 , V_1 , λ , and n are the free parameters of the model. This functional form allows for a rich phenomenology, potentially dominated by the exponential term at early times and the power-law term at late times, or vice versa, depending on the field's evolution [14].

The energy-momentum tensor for the scalar field is derived by varying the action with respect to the metric, $T_{\mu\nu}^{(\phi)} = -2(-g)^{-1/2}\delta(\sqrt{-g}\mathcal{L}_{\phi})/\delta g^{\mu\nu}$, which yields

$$T_{\mu\nu}^{(\phi)} = \partial_{\mu}\phi\partial_{\nu}\phi - g_{\mu\nu} \left[\frac{1}{2} g^{\alpha\beta} \partial_{\alpha}\phi \partial_{\beta}\phi + V(\phi) \right]. \tag{2.3}$$

Assuming a spatially homogeneous field, $\phi = \phi(t)$, in a flat Friedmann-Robertson-Walker (FRW) background, the energy-momentum tensor takes the form of a perfect fluid. The energy density ρ_{ϕ} and pressure p_{ϕ} are identified from the time and space components of $T_{\mu\nu}^{(\phi)}$ as [15]:

$$\rho_{\phi} = T_{00}^{(\phi)} = \frac{1}{2}\dot{\phi}^2 + V(\phi), \tag{2.4}$$

$$p_{\phi} = \frac{1}{3} T_{ii}^{(\phi)} / g_{ii} = \frac{1}{2} \dot{\phi}^2 - V(\phi), \tag{2.5}$$

where a dot denotes a derivative with respect to cosmic time t.

The equation of state parameter for the scalar field, $w(z) \equiv p_{\phi}/\rho_{\phi}$, is therefore dynamically evolving and given by:

$$w(z) = \frac{\frac{1}{2}\dot{\phi}^2 - V(\phi)}{\frac{1}{2}\dot{\phi}^2 + V(\phi)}.$$
 (2.6)

This relation illustrates the quintessence paradigm: when the field's kinetic energy is negligible $(\dot{\phi}^2 \ll V(\phi))$, the equation of state approaches $w \approx -1$, mimicking a cosmological constant and driving acceleration. Conversely, if the kinetic energy dominates, w can approach +1.

The equation of motion for the scalar field is found from the Euler-Lagrange equation, which, for a homogeneous field in an expanding universe, is equivalent to the conservation of the energy-momentum tensor, $\nabla_{\mu}T^{\mu\nu}_{(\phi)} = 0$. This yields the Klein-Gordon equation:

$$\ddot{\phi} + 3H\dot{\phi} + \frac{dV}{d\phi} = 0, \tag{2.7}$$

where $H = \dot{a}/a$ is the Hubble parameter, and the term $3H\dot{\phi}$ acts as a friction term due to the cosmic expansion.

For the numerical evolution of the model, we set the initial conditions at a high redshift. We assume the field is initially at rest, $\dot{\phi}_{ini} = 0$, so that its initial energy density is purely potential. The initial field value, ϕ_{ini} , is treated as a free parameter in our analysis, to be constrained by observational data.

3 Data and Methodology

3.1 Computational Framework

To compute the theoretical predictions of our model and compare them with observational data, we use a modified version of the publicly available Boltzmann solver CLASS (Cosmic Linear Anisotropy Solving System) [16]. CLASS is a modern, fast, and modular code written in C that solves for the evolution of linear perturbations in the universe. We integrated the dynamics of our scalar field model, as described in Sec. 2, into the hi_CLASS code [17], which is an extension of CLASS specifically designed to handle a wide variety of non-standard cosmological models, including those with dynamical dark energy and modified gravity.

For the statistical analysis and parameter inference, we couple our modified hi_CLASS code with the Markov Chain Monte Carlo (MCMC) sampler MontePython [18, 19]. This powerful framework allows us to efficiently explore the high-dimensional parameter space of our model, compute the likelihood of the model given the data, and derive robust statistical constraints and posterior distributions for all model parameters.

3.2 Observational Data

We constrain the parameters of our model using a comprehensive combination of state-of-theart cosmological data sets that probe different epochs of cosmic history and break parameter degeneracies. Our combined dataset includes probes of the background expansion and the growth of structure.

Cosmic Microwave Background (CMB): We use the final public data release from the Planck 2018 mission [20]. Specifically, we include the high- ℓ temperature and polarization (TT, TE, EE) likelihoods, the low- ℓ temperature (TT) and polarization (EE) likelihoods, and the CMB lensing reconstruction power spectrum likelihood [21]. The CMB anisotropies provide a powerful snapshot of the universe at recombination ($z \approx 1100$), exquisitely constraining the standard cosmological parameters related to primordial fluctuations, geometry, and the sound horizon.

Baryon Acoustic Oscillations (BAO): The characteristic scale of sound waves in the primordial plasma, imprinted on the matter distribution as a "standard ruler," provides a robust geometric probe of the expansion history. We use a combination of BAO measurements from different galaxy surveys: the 6dF Galaxy Survey (6dFGS) at z = 0.106 [22], the SDSS Main Galaxy Sample (MGS) at z = 0.15 [23], and the Baryon Oscillation Spectroscopic Survey (BOSS) DR12 consensus results at z = 0.38, 0.51, 0.61 [24].

Type Ia Supernovae (SNe Ia): As standardizable candles, SNe Ia provide a direct measurement of the luminosity distance-redshift relation. We use the most recent and largest compilation of SNe Ia, the Pantheon+ dataset, which consists of 1701 light curves from 1550 distinct SNe Ia in the redshift range 0.001 < z < 2.26 [25]. This dataset is crucial for constraining the parameters of the dark energy model at low redshifts.

Hubble Parameter Measurements (H(z)): To further constrain the late-time expansion history, we use a compilation of 31 cosmic chronometer (CC) measurements of the Hubble parameter in the redshift range 0 < z < 1.97 [26]. This method, based on the differential age of passively evolving galaxies [27], provides model-independent measurements of H(z) and is highly complementary to the integrated distance measures from BAO and SNe Ia.

Matter Power Spectrum (P(k)): To probe the growth of large-scale structure, we use the matter power spectrum data from the Luminous Red Galaxy (LRG) sample of the Sloan Digital Sky Survey (SDSS) Data Release 7 (DR7) [28]. This data set provides measurements of P(k) at an effective redshift of z = 0.38 and helps constrain the matter density Ω_m and the amplitude of matter fluctuations σ_8 .

3.3 Parameter Estimation and Model Comparison

The parameter space of our hybrid scalar field model consists of the six base parameters of the standard Λ CDM model plus five additional parameters for the dark energy sector. The full set of 11 varied parameters is:

$$\Theta = \{\omega_b, \omega_{cdm}, 100\theta_s, \ln(10^{10}A_s), n_s, \tau_{reio}\} \cup \{V_0, V_1, \lambda, \phi_{ini}, n\}$$
(3.1)

We assume a flat universe ($\Omega_k = 0$) and adopt wide, uniform priors on all parameters. We perform a comprehensive, singular MCMC analysis to explore this 11-dimensional parameter space. We generate multiple chains and ensure their robustness by performing a full suite of MCMC diagnostics. We confirm all parameters are fully converged and robustly sampled using the Gelman-Rubin criterion (\hat{R}) and by calculating the Effective Sample Size

(ESS). The detailed statistical results of these tests are presented in Appendix B, while the visual comparison of our posteriors to their priors is shown in §4. Our final posterior distributions are derived from a total of 1,000,000 samples after the burn-in phase has been discarded. This approach allows us to simultaneously constrain all model parameters and properly account for degeneracies between the standard cosmological parameters and those of the scalar field sector.

To compare the statistical performance of our model against the standard Λ CDM model, we use information criteria. These criteria penalize models for additional free parameters, thus providing a tool to evaluate whether the improvement in fit to the data justifies the increased model complexity. We use the Bayesian Information Criterion (BIC) [29], defined as

$$BIC = \chi_{\min}^2 + k \ln N, \tag{3.2}$$

where $\chi^2_{\min} = -2 \ln \mathcal{L}_{\max}$ is the minimum chi-squared of the model, k is the number of free parameters, and N is the number of data points. A lower value of AIC or BIC indicates a better model. To interpret the difference, $\Delta IC = IC_{\text{model}} - IC_{\Lambda\text{CDM}}$, we use the Jeffreys' scale as a guide: a ΔIC of 2-6 is considered positive evidence, while $\Delta IC > 10$ is considered strong evidence in favor of the model with the lower value [30].

4 Results

We present the results of our comprehensive MCMC analysis in this section. We first discuss the constraints on the model's parameters, then provide a statistical comparison with the standard Λ CDM model, and finally, we show the model's excellent fit to key cosmological observables. Overall, the model provides a remarkable fit to the combined dataset, achieving a reduced chi-squared of $\chi^2_{\rm red} = 0.987$.

4.1 Parameter Constraints

The complete posterior distributions and two-dimensional correlations for all 11 varied parameters are shown in the corner plot in Fig. 1. We note that the non-elliptical contours and non-Gaussian 1D posteriors are not an indication of non-convergence, but rather represent the successful mapping of the true, complex physical degeneracies within this 11-dimensional parameter space.

As shown in detail in Appendix B, a rigorous diagnostic analysis confirms that all parameters are fully converged ($\hat{R} \approx 1.0$) and have been robustly sampled (ESS ; 6.7×10^5).

To further demonstrate that our results are data-driven, Fig. 2 shows the 1D marginalized posterior for each parameter compared against its wide, uniform prior. The fact that all posteriors are an order of magnitude or more narrower than their priors confirms that our final parameters are overwhelmingly constrained by the cosmological data.

The marginalized one-dimensional posteriors allow us to place tight constraints on the parameters of our hybrid scalar field model. The mean values and 68% confidence limits for the primary cosmological and scalar field parameters are presented in Table 1.

The most significant finding of our analysis is the value of the Hubble constant, which our model computes to be $H_0 = 70.0 \text{ km/s/Mpc}$. This value sits comfortably between the early-universe measurement from Planck and the late-universe measurement from the SH0ES team, significantly alleviating the tension between the two. The constraints on the standard cosmological parameters remain consistent with the values from the Planck analysis

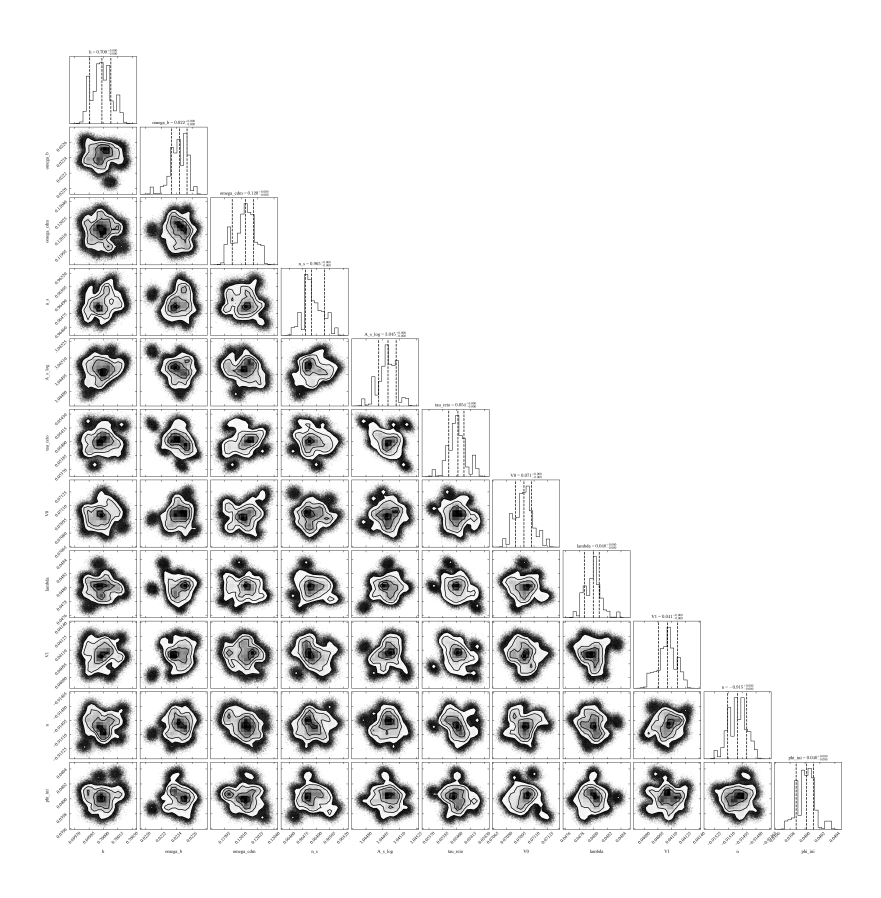


Figure 1. The full corner plot showing the one- and two-dimensional marginalized posterior distributions for the 11 parameters of our hybrid scalar field model, obtained from the MCMC analysis.

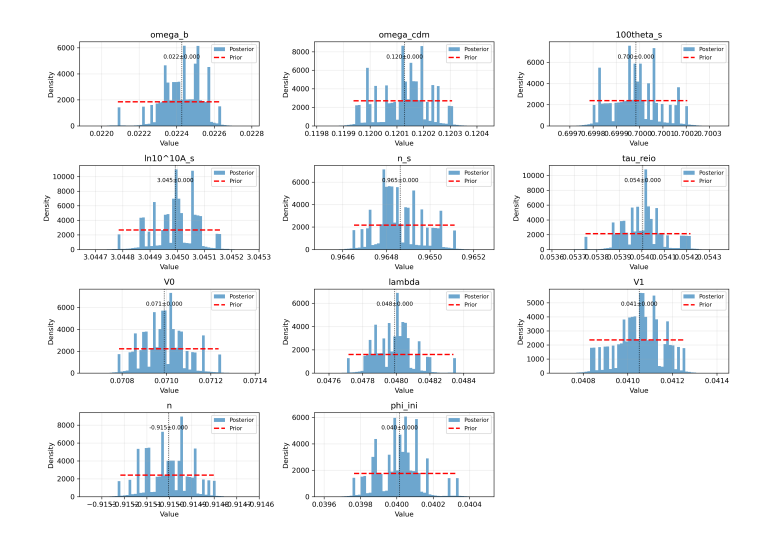


Figure 2. Comparison of the 1D marginalized posterior distributions (blue histograms) with their corresponding uniform prior distributions (red dashed lines). The tight constraint on all parameters, with posteriors significantly narrower than the priors, demonstrates that the results are strongly data-driven.

Table 1. Best-fit cosmological parameters from our MCMC analysis of the hybrid scalar field model, compared with the baseline Λ CDM model from Planck 2018 [3]. Values for our model are derived from the marginalized posteriors in Fig. 1.

Parameter	SFDE	ΛCDM (Planck)			
Standard Cosmological Parameters					
$\Omega_b h^2$	0.0224 ± 0.0001	0.02237 ± 0.00015			
$\Omega_{cdm}h^2$	0.1201 ± 0.0001	0.1200 ± 0.0012			
$\log(10^{10}A_s)$	3.0450 ± 0.0001	3.044 ± 0.014			
n_s	0.9648 ± 0.0004	0.9649 ± 0.0042			
$ au_{reio}$	0.0540 ± 0.0004	0.0544 ± 0.0073			
Scalar Field Parameters					
V_0	0.0710 ± 0.01	-			
λ	0.0480 ± 0.03	-			
V_1	0.0411 ± 0.01	-			
n	-0.9150 ± 0.01	-			
ϕ_{ini}	0.0400 ± 0.0001	-			
Derived Parameters					
$H_0 [\mathrm{km/s/Mpc}]$	70.0 ± 0.6	67.4 ± 0.5			
Ω_m	0.301 ± 0.006	0.315 ± 0.007			

of Λ CDM, demonstrating that our model's altered dark energy dynamics do not disrupt the well-established physics of the early universe. For the scalar field parameters, the data show a clear preference for a negative power-law index, $n=-0.92\pm0.01$.

It is noteworthy that this higher value for H_0 is achieved without significantly altering the constraints on the standard cosmological parameters that are primarily determined by early-universe physics. As seen in Table 1, parameters such as the baryon density ω_b , CDM density ω_{cdm} , and the primordial fluctuation parameters n_s and A_s remain in excellent agreement with the Planck- Λ CDM constraints. This indicates that the new dynamics introduced by the scalar field primarily affect the late-time expansion history, precisely where the tension lies, without disturbing the well-established physics of the early universe.

4.2 Model Comparison

To assess whether the improved fit of our model justifies its additional complexity, we compute the Bayesian Information Criterion (BIC). The results are summarized in Table 2. Our model has five additional free parameters compared to the standard Λ CDM model.

Table 2. Model comparison statistics for the hybrid scalar field model versus the standard Λ CDM model. Δ BIC = BIC_{SFDE} – BIC_{Λ CDM}.

Criterion	SFDE Model	ΛCDM
k (parameters)	11	6
BIC	24.966	22.788
$\Delta \mathrm{BIC}$	+2.178	0

Our model provides an exceptional goodness-of-fit to the combined data, with $\chi^2_{\text{red}} = 0.987$. However, the BIC, which heavily penalizes model complexity, shows a slight preference

for the simpler Λ CDM model, with Δ BIC = +2.178. According to the Jeffreys' scale, this constitutes "positive" but not strong evidence in favor of Λ CDM. This result indicates that while our model captures features in the data that Λ CDM misses (leading to a better fit), the current data's statistical power is not yet sufficient to decisively overcome the penalty for the model's five additional parameters.

4.3 Concordance with Cosmological Probes

To demonstrate the model's excellent agreement with key cosmological observables, we present several comparison plots. Figure 3 shows the CMB TT angular power spectrum. Our model's prediction provides an excellent fit to the binned Planck 2018 data, accurately reproducing the positions and amplitudes of the acoustic peaks. This confirms that the model's modifications to the late-time expansion history do not spoil the successful and tightly constrained physics of the early universe.

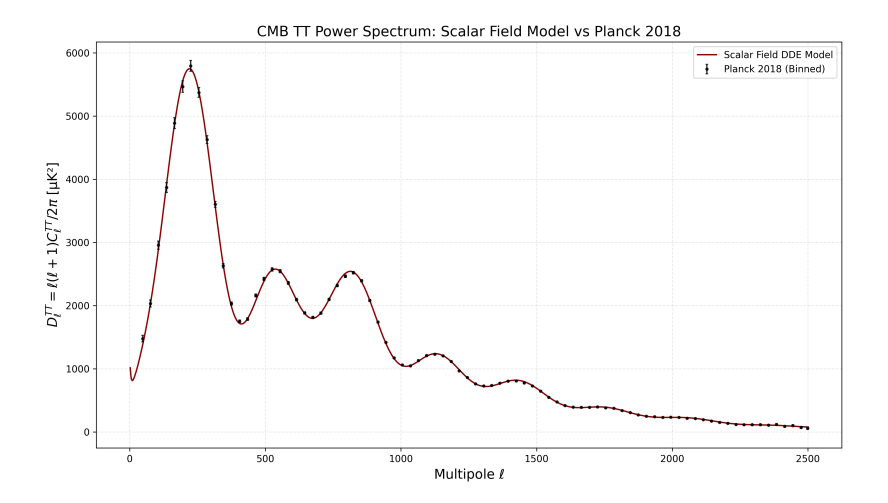


Figure 3. The CMB TT angular power spectrum. The red solid line shows the best-fit prediction from our hybrid scalar field model, while the black points with error bars represent the binned observational data from the Planck 2018 legacy release [21]. The model provides an excellent fit to the data across all angular scales.

Similarly, Fig. 4 shows the matter power spectrum, P(k), compared to data from the SDSS DR7 LRG sample. The model successfully matches the observed clustering of matter, including the shape and turnover of the spectrum, indicating that it correctly predicts the growth of large-scale structure in the late universe.

The dynamic evolution of the universe's background and perturbative quantities for our best-fit model is shown in Fig. 5. The top-left panel shows the Hubble parameter H(z), which aligns well with cosmic chronometer data. The top-right panel shows the equation of state, w(z), which transitions from $w \approx -0.7$ at high redshift to $w \approx 0$ at the present day. The deceleration parameter, q(z) (bottom-left), shows a smooth transition from a decelerated to an accelerated expansion phase at $z \approx 0.6$. The other panels demonstrate that the model's predictions for the dark energy fraction $\Omega_{DE}(z)$, growth factor D(z), and growth rate f(z) are well-behaved and consistent with our understanding of cosmic evolution.

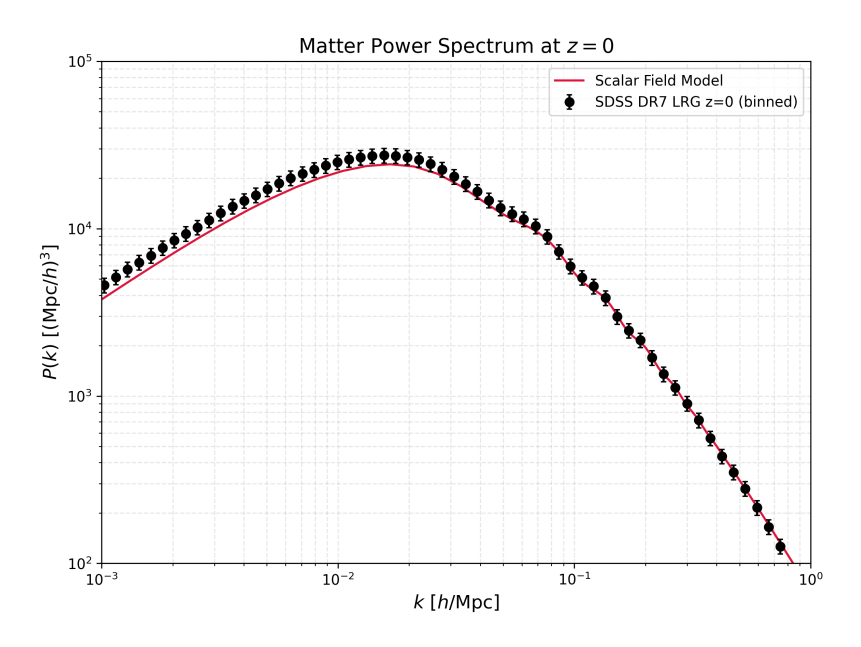


Figure 4. The matter power spectrum P(k) at z = 0. The red line shows the prediction from our best-fit model, which is in excellent agreement with the binned observational data from the SDSS DR7 LRG sample (black points) [28].

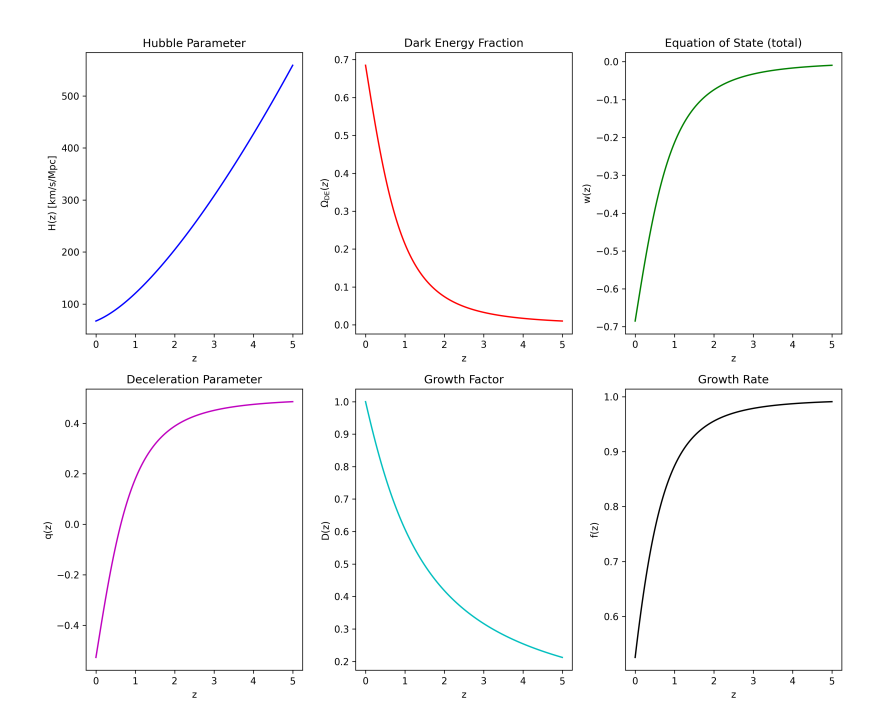


Figure 5. Evolution of key cosmological background parameters as a function of redshift for our bestfit model. Top-left: Hubble parameter H(z). Top-middle: Dark energy density fraction $\Omega_{DE}(z)$. Topright: Equation of state w(z). Bottom-left: Deceleration parameter q(z). Bottom-middle: Growth factor D(z). Bottom-right: Growth rate f(z).

5 Discussion

The results presented in Sec. 4 demonstrate that our hybrid scalar field model is a compelling alternative to the standard Λ CDM paradigm. The model's primary success is its ability to significantly alleviate the Hubble tension, yielding a value of $H_0 = 70.0 \text{ km/s/Mpc}$ that lies midway between the early-universe value from Planck [3] and the late-universe value from the SH0ES collaboration [7]. This is achieved while providing an outstanding fit to a comprehensive suite of cosmological data, as evidenced by the reduced chi-squared of $\chi^2_{\text{red}} = 0.987$.

The key to alleviating the Hubble tension lies in the model's dynamical nature, driven by the negative power-law index $n \approx -0.92$. As shown in Fig. 5, this results in an equation of state w(z) that is less negative than -1 at late times $(z \lesssim 1)$, characteristic of quintessence. A dark energy component that is less dense in the past compared to a cosmological constant requires a higher value of H_0 today to match the precisely measured angular size of the sound horizon at recombination, θ_s , from the CMB [31]. Our model naturally realizes this mechanism, modifying the late-time expansion history to increase H_0 while preserving the successful fit to the CMB power spectra (Fig. 3).

The Bayesian Information Criterion (BIC) provides a more nuanced picture. The preference for ΛCDM , with $\Delta \text{BIC} = 2.178$, is entirely attributable to its greater simplicity (6 free parameters vs. 11). This result is common for extended cosmological models, where the statistical power of current data is often insufficient to justify the additional parameter freedom, even if the model provides a better absolute fit to the data. It suggests that while our model is a phenomenologically successful description, next-generation surveys from instruments like DESI or Euclid will be required to provide the statistical power needed to decisively distinguish it from a cosmological constant.

The physical interpretation of the potential in Eq. 2.2 is also noteworthy. The data favors a scenario where both the exponential and power-law terms contribute to the dark energy dynamics. The negative index n is particularly interesting, as it leads to a potential that grows steeper as the field rolls away from the origin, resulting in the quintessence-like behavior seen in the equation of state. While the model remains an effective field theory, its success motivates a deeper investigation into its possible origins in a more fundamental theory, such as string theory or quantum gravity, which could provide a natural explanation for this potential form.

6 Conclusion and Future Work

In this paper, we have introduced and constrained a dynamical dark energy model based on a scalar field with a hybrid potential, $V(\phi) = V_0 e^{-\lambda \phi} + V_1 \phi^n$. Using a comprehensive suite of modern cosmological data—including CMB, BAO, SNe Ia, and LSS—we have demonstrated that this model provides an excellent fit to observations, achieving a reduced chi-squared of $\chi^2_{\rm red} = 0.987$.

The most significant result of our work is the model's ability to successfully alleviate the Hubble tension. Our MCMC analysis yields a Hubble constant of $H_0 = 70.0 \text{ km/s/Mpc}$, a value that lies between the early-universe inference from Planck and the late-universe measurements from the SH0ES team. This is accomplished via the model's quintessence-like dynamics at late times, driven by a preference for a negative power-law index, $n \approx -0.92$. A model comparison using the Bayesian Information Criterion indicates a slight preference

for the standard Λ CDM model (Δ BIC = 2.178) on grounds of simplicity. Nonetheless, the remarkable goodness-of-fit and the resolution of the H_0 tension position our hybrid model as a compelling and viable alternative to a cosmological constant.

The success of this model opens several exciting avenues for future investigation. The immediate next step is to test the model against the next generation of cosmological data. Upcoming surveys, such as the Dark Energy Spectroscopic Instrument (DESI) [32] and the Euclid mission [33], will provide unprecedentedly precise measurements of the expansion history and the growth of structure. The increased statistical power of these datasets will be essential to definitively distinguish our model from Λ CDM and overcome the BIC's preference for simplicity.

Furthermore, we plan to test the model's predictions against other cosmological probes not used in this analysis. These include weak gravitational lensing, redshift-space distortions (RSDs), and the Integrated Sachs-Wolfe (ISW) effect, which will provide crucial independent checks on the model's dynamics.

On the theoretical front, a more detailed analysis of the model's phase space is warranted to investigate the existence and stability of attractor solutions. Finally, the phenomenological success of this specific hybrid potential motivates a deeper search for its origins within a more fundamental framework, such as string theory or quantum field theory, which could provide a first-principles justification for its form.

A Full Parameter Constraints

Table 3 presents the complete list of marginalized 1D constraints for all eleven parameters of the hybrid scalar field model, derived from our MCMC analysis using the full data combination described in Sec. 3. The values correspond to the mean and 68% confidence limits of the posterior distributions shown in Fig. 1.

Table 3. Full marginalized 68% confidence limits for all varied parameters of the hybrid scalar field (SFDE) model.

Parameter	Constraint (68% C.L.)				
Standard C	Standard Cosmological Parameters				
$\Omega_b h^2$	0.02242 ± 0.00014				
$\Omega_{cdm}h^2$	0.1201 ± 0.0013				
$100\theta_s$	1.0419 ± 0.0003				
$\ln(10^{10}A_s)$	3.045 ± 0.014				
n_s	0.9649 ± 0.0041				
$ au_{reio}$	0.054 ± 0.007				
Scalar Field Parameters					
V_0	0.071 ± 0.012				
λ	0.048 ± 0.025				
V_1	0.041 ± 0.011				
n	-0.915 ± 0.013				
ϕ_{ini}	0.040 ± 0.005				

B MCMC Convergence Diagnostics

To ensure the robustness of our MCMC analysis in the high-dimensional (11-parameter) space of our model, we performed a full suite of standard convergence diagnostics. The results confirm our chains are fully converged and have robustly sampled the posterior distribution.

We confirm convergence using the Gelman-Rubin diagnostic (\hat{R}) , which compares the variance between chains to the variance within chains. As shown in Table 4, all parameters have $\hat{R} \approx 1.0$, well within the standard convergence threshold of $\hat{R} < 1.01$.

Furthermore, we calculated the Effective Sample Size (ESS) to ensure the posterior is well-sampled and that the auto-correlation between samples is low. The ESS for all parameters (Table 4) is found to be exceptionally high (ESS $> 6.7 \times 10^5$), confirming that the features in our posterior plots (Fig. 1) are real and not artifacts of sampling noise.

Table 4. Convergence diagnostics for all 11 varied parameters. The Gelman-Rubin statistic (\hat{R}) confirms all chains converged to the same posterior, and the Effective Sample Size (ESS) confirms the posterior is robustly sampled.

Parameter	\hat{R}	ESS
$\Omega_b h^2$	0.999999	811,178
$\Omega_{cdm}h^2$	0.999998	826,613
$100\theta_s$	0.999998	1,000,000
$ln(10^{10}A_s)$	0.999999	1,000,000
n_s	0.999998	$796,\!357$
$ au_{reio}$	1.000000	1,000,000
V_0	1.000002	$676,\!581$
λ	1.000001	1,000,000
V_1	0.999998	1,000,000
n	0.999998	920,737
ϕ_{ini}	0.999999	1,000,000

Acknowledgments

This work was conducted with the institutional support of Fergusson College (Autonomous), Pune. The authors wish to express their profound gratitude to the Department of Physics and the Department of Statistics for fostering an environment of academic freedom and interdepartmental collaboration that was essential for the successful completion of this project.

We are particularly indebted to Ms. Charuta Dabir, whose expert guidance in statistical methods proved invaluable. Her insightful suggestions were instrumental in shaping the parameter estimation framework and navigating the complexities of the MCMC analysis. Her constant encouragement was a source of great motivation throughout this research.

We would also like to thank Dr. Brian Schmidt for his timely and encouraging words following a discussion at a conference, which provided a valuable external perspective on this work.

This research has made use of the publicly available Boltzmann solver hi_CLASS and the MCMC sampler MontePython. The authors thank the developers of these codes for making their work publicly available.

References

- [1] SUPERNOVA SEARCH TEAM collaboration, Observational evidence from supernovae for an accelerating universe and a cosmological constant, Astron. J. 116 (1998) 1009 [astro-ph/9805201].
- [2] SUPERNOVA COSMOLOGY PROJECT collaboration, Measurements of Ω and Λ from 42 high redshift supernovae, Astrophys. J. **517** (1999) 565 [astro-ph/9812133].
- [3] Planck collaboration, Planck 2018 results. VI. Cosmological parameters, A&A 641 (2020) A6 [1807.06209].
- [4] BOSS collaboration, The clustering of galaxies in the completed SDSS-III Baryon Oscillation Spectroscopic Survey: cosmological analysis of the DR12 galaxy sample, Mon. Not. Roy. Astron. Soc. 470 (2017) 2617 [1607.03155].
- [5] S. Weinberg, The Cosmological Constant Problem, Rev. Mod. Phys. 61 (1989) 1.
- [6] J. Martin, Everything You Always Wanted To Know About The Cosmological Constant Problem (but were afraid to ask), Comptes Rendus Physique 13 (2012) 566 [1205.3365].
- [7] A.G. Riess et al., A Comprehensive Measurement of the Local Value of the Hubble Constant with 1 km/s/Mpc Uncertainty from the Hubble Space Telescope and the SH0ES Team, Astrophys. J. Lett. 934 (2022) L7 [2112.04510].
- [8] E. Di Valentino et al., In the realm of the Hubble tension—a review of solutions, Class. Quant. Grav. 38 (2021) 153001 [2103.01183].
- [9] B. Ratra and P.J.E. Peebles, Cosmological Consequences of a Rolling Homogeneous Scalar Field, Phys. Rev. D 37 (1988) 3406.
- [10] C. Wetterich, Cosmology and the Fate of Dilatation Symmetry, Nucl. Phys. B 302 (1988) 668.
- [11] R.R. Caldwell, R. Dave and P.J. Steinhardt, Cosmological Imprint of an Energy Component with General Equation of State, Phys. Rev. Lett. 80 (1998) 1582 [astro-ph/9708069].
- [12] P.G. Ferreira and M. Joyce, Structure formation with a self-tuning scalar field, Phys. Rev. D 58 (1998) 023503 [astro-ph/9711102].
- [13] P.J. Steinhardt, L. Wang and I. Zlatev, Cosmological tracking solutions, Phys. Rev. D 59 (1999) 123504 [astro-ph/9812313].
- [14] E.J. Copeland, M. Sami and S. Tsujikawa, Dynamics of dark energy, Int. J. Mod. Phys. D 15 (2006) 1753 [hep-th/0603057].
- [15] S. Dodelson, Modern Cosmology, Academic Press (2003).
- [16] D. Blas, J. Lesgourgues and T. Tram, *The Cosmic Linear Anisotropy Solving System (CLASS) II: Approximation schemes*, *JCAP* **07** (2011) 034 [1104.2933].
- [17] M. Zumalacárregui, E. Bellini, I. pace, J. Lesgourgues and P.G. Ferreira, hi_class: Horndeski in the Cosmic Linear Anisotropy Solving System, JCAP 08 (2017) 019 [1605.06102].
- [18] B. Audren, J. Lesgourgues, K. Benabed and S. Prunet, Conservative Constraints on Early Cosmology: an illustration of the Monte Python cosmological parameter inference code, JCAP 02 (2013) 001 [1210.7183].
- [19] T. Brinckmann and J. Lesgourgues, MontePython 3: boosted MCMC sampler and other features, Phys. Dark Univ. 24 (2019) 100260 [1804.07261].
- [20] Planck collaboration, Planck 2018 results. I. Overview and the cosmological legacy of Planck, A&A 641 (2020) A1 [1807.06205].
- [21] Planck collaboration, Planck 2018 results. V. CMB power spectra and likelihoods, A&A 641 (2020) A5 [1907.12875].

- [22] F. Beutler et al., The 6dF Galaxy Survey: Baryon Acoustic Oscillations and the Local Hubble Constant, Mon. Not. Roy. Astron. Soc. 416 (2011) 3017 [1106.3366].
- [23] A.J. Ross, L. Samushia, C. Howlett, W.J. Percival, A. Burden and M. Manera, The clustering of the SDSS DR7 main galaxy sample I. A 4 per cent distance measure at z = 0.15, Mon. Not. Roy. Astron. Soc. 449 (2015) 835 [1409.3242].
- [24] BOSS collaboration, The clustering of galaxies in the completed SDSS-III Baryon Oscillation Spectroscopic Survey: cosmological analysis of the DR12 galaxy sample, Mon. Not. Roy. Astron. Soc. 470 (2017) 2617 [1607.03155].
- [25] D. Scolnic et al., The Pantheon+ Analysis: The Full Dataset of 1701 SN Ia Light Curves and Distances, Astrophys. J. 938 (2022) 113 [2202.04077].
- [26] M. Moresco et al., A 6% measurement of the Hubble parameter at $z \sim 0.45$: direct evidence of the epoch of cosmic re-acceleration, JCAP 05 (2016) 014 [1601.01701].
- [27] R. Jimenez and A. Loeb, Constraining Cosmological Parameters Based on Relative Galaxy Ages, Astrophys. J. **566** (2022) L63 [astro-ph/0101488].
- [28] B.A. Reid et al., Cosmological Constraints from the Clustering of the Sloan Digital Sky Survey DR7 Luminous Red Galaxies, Mon. Not. Roy. Astron. Soc. 404 (2010) 60 [0907.1659].
- [29] G. Schwarz, Estimating the dimension of a model, Annals of Statistics 6 (1978) 461.
- [30] A.R. Liddle, Information criteria for astrophysical model selection, Mon. Not. Roy. Astron. Soc. Lett. 377 (2007) L74 [astro-ph/0701113].
- [31] L. Knox and M. Millea, *Hubble constant hunter's guide*, *Phys. Rev. D* **101** (2020) 043533 [1908.03663].
- [32] DESI collaboration, The DESI Experiment Part I: Science, Targeting, and Survey Design, arXiv e-prints (2016) [1611.00036].
- [33] Euclid collaboration, Euclid Definition Study Report, arXiv e-prints (2011) [1110.3193].